JOURNAL OF MATERIALS SCIENCE 33 (1998) 423–427

Strength of β-sialon/Si_3N_4 layered composites

Y. GOTO, T. FUKASAWA, M. KATO
Materials and Devices Research Laboratories, Research and Development Center, Toshiba Corporation 1, Komukai Toshiba-cho, Saiwai-ku, Kawasaki 210, Japan

The strength of layered composites consisting of β-sialon and Si_3N_4 layers, which were prepared by hot pressing, was investigated. The strength increased as the thickness of the sialon (outer layer) decreased, and reached almost the same level of Si_3N_4 (inner layer) when the sialon thickness was 250–300 μm. No specific fracture morphologies were recognized around the interface of sialon and Si_3N_4. The aluminium concentration changed sharply around the interface, while the yttrium tended to diffuse deeper than aluminium. This tendency was remarkable in the samples hot-pressed at higher temperature (1900 °C). The existence of compressive residual stress in the surface sialon layer was revealed and the residual stress increased as the sialon thickness decreased down to 250–300 μm. The increase of strength with the decrease of sialon thickness was discussed based on the mechanical calculations in which the residual stress was considered. This calculation approximately agreed with the results of the samples hot-pressed at lower temperature (1800 °C). However, the strength of the samples hot-pressed at 1900 °C was much higher than the prediction in the thin range of the sialon thickness. The deep diffusion of yttrium into the sialon layers was thought to be one of the causes of this unpredictable effect.

1. Introduction

High-temperature materials are essential to increase the energy conversion efficiency of heat engines (e.g. gas turbines), by raising the operating temperature. In these applications, materials with both high strength and high oxidation resistance are required.

Si_3N_4 ceramics are known to have high strength and good fracture toughness, while the good oxidation resistance of sialon ceramics is greatly superior to that of silicon nitride [1–3]. These properties are attributable to the microstructural differences, i.e. grain shape and secondary grain-boundaries. To obtain ceramics with high strength and good oxidation resistance, we attempted to fabricate layered composites consisting of sialon and Si_3N_4, i.e. the surface layer was β-sialon to protect Si_3N_4 from oxidation. Thermal mismatches of these ceramics were estimated to be small, because these two ceramics are chemically very close, as sialon is formed by the aluminium solid-solution into Si_3N_4 [4, 5].

In recent years, ceramic layered composites have been studied. The fabrication of multilayered composites of Al_2O_3/ZrO_2 [6, 7] and Al_2O_3/TiO_2 [8] were tried by slip casting. Functionally gradient composites of Al_2O_3/YTZP [9] and Al_2O_3/Al_2TiO_5 [10] were obtained by sequential slip casting. There has also been some research into the fracture behaviour and toughening mechanisms of multilayer composites [11–14]. In addition, research into the strength of ceramic layered composites has been reported [15–18]. Particularly, composites with compressive surface residual stress showed higher strength than those with no residual stress. To realize the compressive residual stress in the surface layer, three-layer composites of ($Al_2O_3 + ZrO_2$ (unstabilized))/($Al_2O_3 + ZrO_2$ (stabilized)) [15–17] and (SiC + AlN(10%))/(SiC + AlN(50%)) [18] have been investigated.

However, there have been few reports on sialon/Si_3N_4 layered composites. In these layered composites, strength behaviour is thought to be the most important issue, because the surface sialon, which has lower strength at room temperature and in a lower temperature range than Si_3N_4, may govern the strength of the composites. In this work, therefore, the focus was on the strength of the layered composites, and the oxidation behaviour was left for further investigations. To simplify the experiments, two-layer composites of sialon and Si_3N_4 were studied.

2. Experimental procedure

β-sialon/Si_3N_4 layered composites were fabricated by hot-pressing. The starting powders were prepared by ball-mill mixing a commercial-grade Si_3N_4 powder (E-10, Ube Industry Co. Ltd., Tokyo, Japan) with 10 wt% Al_2O_3 for the β-sialon layer and with 2 wt% Al_2O_3 and 5 wt% Y_2O_3 for the Si_3N_4 layer. Because the starting composition of the sialon was only Si_3N_4 and Al_2O_3, the oxygen content slightly exceeded the exact sialon composition. However, β-sialon was detected as a single phase by X-ray diffraction and good strength (about 600 MPa) was already confirmed [19–21]. The composition of sintering aids for Si_3N_4 was a typical one for high-strength Si_3N_4 [22, 23]. The

0022–2461

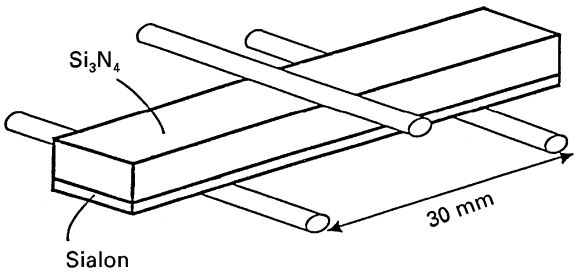

Figure 1 Bending strength measurement of the layered composites.

ball-mill mixing was performed for 24 h using *n*-butanol as a liquid medium. After drying, the powders were cold-pressed at a pressure of 60 MPa to shape the two-layered green compacts. Hot-pressing was done in a carbon die at temperatures of 1800 or 1900 °C and at a pressure of 40 MPa for 60 min. The hot-pressing atmosphere was 0.1 MPa N_2 for 1800 °C hot-pressing and 0.7 MPa N_2 for 1900 °C hot-pressing to suppress the decomposition of Si_3N_4. Monolithic β-sialon and Si_3N_4 were fabricated under the same conditions for comparison. Consolidation was confirmed by density measurement using the Archimedes method with water immersion. The densities of the monolithic and composite specimens were determined to be more than 99% of full density for both 1800 and 1900 °C hot-pressing.

Specimens for bending strength measurement were cut from the hot-pressed samples so that the stress direction was perpendicular to the hot-pressing direction. The size of the specimen was 4 mm × 3 mm × 40 mm. The specimen thickness was kept constant (3 mm) but the thickness of the sialon layer was changed from 300 μm to 1200 μm. The specimens were set as shown in Fig. 1 in order to impose the tensile stress on the sialon side. The bending strength measurements were conducted by three-point bending at the span of 30 mm and at the cross-head speed of 0.5 mm min^{-1}. Fracture toughness was measured by four-point bending on single-notched specimens with the same dimensions as the strength-test bar for only the monolithic samples. The notch width and depth were 0.5 mm and 0.75 mm, respectively. The span and the loading conditions were the same as for the strength test.

Microstructures of the composites were characterized by scanning electron microscopy (SEM) for fractured surfaces and composition profiles of aluminium and yttrium were measured by electron probe microanalysis (EPMA) for polished surfaces. Crystalline phases were analysed by X-ray diffraction measurement using CuK_α radiation.

Residual stress in the sialon layers was measured by the $\sin^2\psi$ method [24] using the X-ray diffraction peak of the (3 2 3) plane for the samples hot-pressed at 1800 °C. Young's modulus and Poisson's ratio of the monolithic sialon and Si_3N_4 used for the residual stress calculations were determined by the pulse-echo method [25] using a supersonic wave. The thermal expansion coefficient was measured by laser interferometry [26].

TABLE I Properties of monolithic sialon and Si_3N_4

Specimen	HP temp. (°C)	*E* (GPa)	α (10^{-6} °C^{-1})	σ_f (MPa)	K_{IC} (MPa $m^{1/2}$)
Sialon	1800	270	3.03	600	3.9
	1900	–	–	590	2.4
Si_3N_4	1800	315	3.18	1010	8.3
	1900	–	–	890	8.0

E, Young's modulus; α, thermal expansion coefficient; σ_j, fracture strength; K_{IC}, fracture toughness

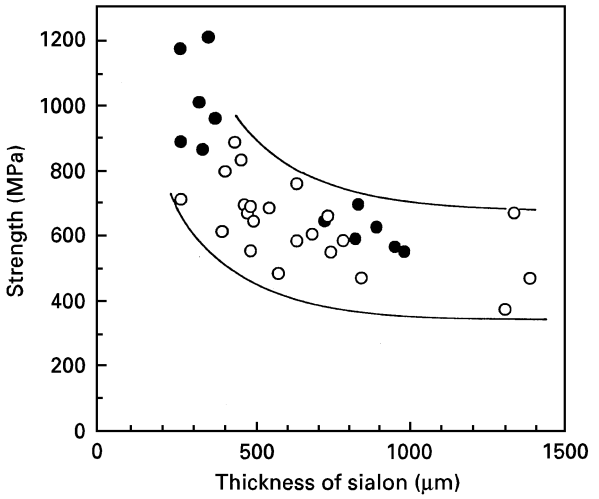

Figure 2 Strength of the layered composites as a function of sialon-layer thickness. Hot-pressing temperature: (○) 1800 °C, (●) 1900 °C.

3. Results and discussion

3.1. Mechanical properties

Young's modulus, thermal expansion coefficient, bending strength, and fracture toughness of the monolithic Si_3N_4 and sialon are listed in Table I, which shows that the mechanical properties of Si_3N_4 were greater than those of sialon. Except for the 1800 °C sialon, which had almost the same level of fracture strength as 1900 °C sialon, 1800 °C samples showed higher strength and toughness than 1900 °C samples.

The relation between the bending strength and the thickness of sialon layer is shown in Fig. 2. The thickness was measured from the fracture surface observation of every test piece to avoid the scattering of the thickness due to the machining. The bending strength was almost constant with decreasing thickness from 1300 μm to approximately 500 μm, and then increased as the thickness decreased further. The strength reached almost the same level as Si_3N_4 (inner layer) when the sialon thickness was 200–300 μm.

3.2. Microstructural characterization

Crystalline phases of β-sialon and β-Si_3N_4 were detected by X-ray diffraction in the sialon layer and Si_3N_4 layer, respectively. No other phases were detected. This means the Si_3N_4 layer had an amorphous grain-boundary phase due to the sintering additives.

Fig. 3 shows the fracture surface of the specimen with a sialon layer of 700 μm hot-pressed at 1800 °C.

Fig. 3a is a low-magnification image and the region marked "1" is enlarged and shown as the micrograph marked "1" in Fig. 3b which shows microstructural changes from the surface sialon to the inner region of Si_3N_4. In this figure, no specific fracture morphologies were recognized, and general aspects of miller, mist, and hackle were observed [27]. It is thought from this observation that the interfaces of sialon and Si_3N_4 were tightly bonded.

Composition of rectangular regions (about 0.5 mm × 2.0 mm) of the cross-sections of the specimens from the sialon surface to the Si_3N_4 layer were analysed by EPMA. Typical results of aluminium and yttrium profiles are shown in Fig. 4 as line profiles of the average counts in the regions from the surface to the inner part of Si_3N_4. In this figure, the aluminium concentration changed sharply in the interface regions, while the yttrium tended to diffuse deeper than aluminium. This tendency was remarkable in the samples hot-pressed at 1900 °C. The aluminium content was higher in the sialon layer than in the Si_3N_4 layer, because the sialon grains contained aluminium as the solid solution. On the other hand, the yttrium content was higher in the Si_3N_4 layer because yttrium came from the sintering additives and existed in the grain-boundary phase. Yttrium seemed to be easier to move through grain boundaries than aluminium.

3.3. Residual stress and discussion of strength

To discuss the strength behaviour of the layered composites, stresses generated in the composite, schematically shown in Fig. 5, were considered in terms of mechanics. The layered composite consist of two layers, 1 and 2, with thickness h_1 and h_2, and Young's modulus E_1 and E_2. The subscripts 1 and 2, indicate each layer. The interface of the layers was assumed to be tightly bonded. When the three-point bending load, P, is imposed on the layered composite with a span of S, because layer 2 is the tension side (shown in Fig. 5), the stresses (σ_1 and σ_2) generated at the bottom of each layer, i.e. the maximum stresses for each layer, are given by [28]

$$\sigma_1 = \frac{E_1(z_0 - h_2)}{E_1 I_1 + E_2 I_2} M \quad (1)$$

$$\sigma_2 = \frac{E_2 z_2}{E_1 I_1 + E_2 I_2} M \quad (2)$$

where M is bending moment which is shown by

$$M = \frac{1}{4} PS \quad (3)$$

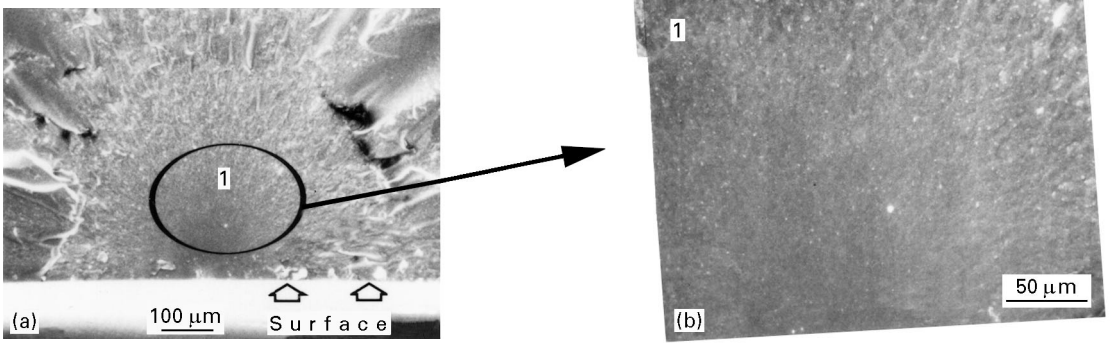

Figure 3 Scanning electron micrographs of the fracture surface for the sample hot-pressed at 1800 °C.

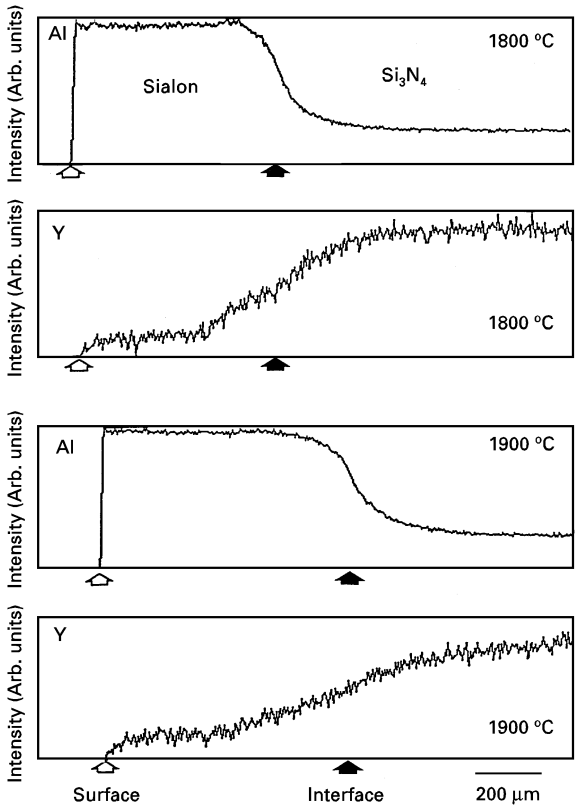

Figure 4 Composition profiles of yttrium and aluminium for the sample hot-pressed at 1800 °C.

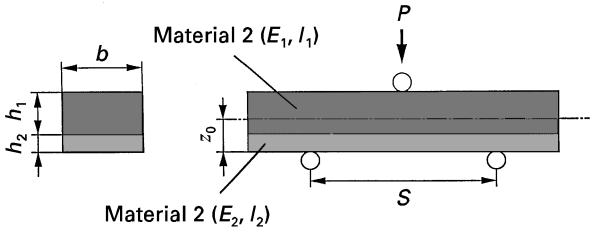

Figure 5 Schematic drawing of a layered composite for strength calculation.

z_0 shows the position of the neutral plane on which there is no stress. It is shown by

$$z_0 = \frac{E_1(h_1 + 2h_1h_2) + E_2h_2^2}{2} \quad (4)$$

I_1 and I_2 are moments of inertia of area which are calculated from

$$I_1 = \frac{b}{3}[(h_1 + h_2 - z_0)^3 - (h_2 - z_0)^3] \quad (5)$$

$$I_2 = \frac{b}{3}[(h_2 - z_0)^3 + z_0^3] \quad (6)$$

Regarding layer 1 as Si_3N_4 and layer 2 as β-sialon, the bending strength of the layered composites was calculated from Equation 2 assuming that the composites would fracture when σ_2 reached the strength of the monolithic sialon (600 MPa). The thickness of the composite and the span used in this calculation were the same as those in the experiment (3 and 30 mm, respectively). The calculated strength was plotted as

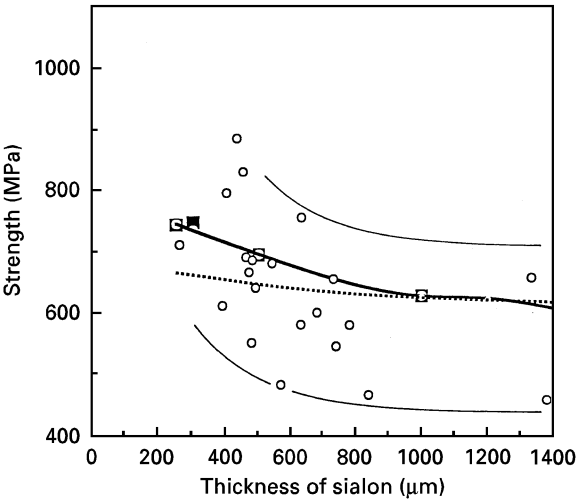

Figure 6 Calculated strengths of layered composites hot-pressed at 1800 °C. (——) Calculated (residual stress), (- - - -) calculated, (○) experimental, (■) calculated (measured residual stress).

TABLE II Residual stress in the sialon layer: σ_R, residual stress; compression stress is shown by negative values

Thickness (μm)	σ_R (measured) (MPa)	σ_R (calculated) (MPa)
250	−70.1	−71.7
300	−77.9	−66.3
500	−44.6	−45.5
1000	−3.0	−2.9

a function of the sialon-layer thickness, h_2, which is shown as the dotted line in Fig. 6. The calculated strength increased slightly with decreasing sialon-layer thickness, but the experimental strength increased more than this calculated result. Then, residual stress was considered in the calculation.

The residual stress in the sialon layer was measured by the X-ray method and calculated [29] from the thermal expansion coefficient, Young's modulus (shown in Table I), Poisson's ratios (0.27 for both sialon and Si_3N_4), thickness of the sialon layer (total thickness was 3 mm), and a temperature difference of 1780 °C (the hot-pressing temperature was 1800 °C). The result of the residual stress measurement is shown in Table II and calculated results corresponding to the measured results are also listed for comparison. This revealed that the existence of compressive residual stress in the surface sialon layer and the calculated values agreed fairly well with the measured values. The compressive stress increased as the sialon thickness decreased down to 250–300 μm corresponding to the strength change with the sialon thickness.

Considering the residual stress, the strength of the layered composite was calculated again, that is, the composite would fracture when the value of σ_2 minus the residual stress reached the strength of the monolithic sialon. The other assumptions were the same as for the previous calculation. The result of this calculation is shown in Fig. 6 as the solid line, which is derived from the calculated residual stress, and the closed squares, which are derived from the measured residual stress. In this figure, experimental data of the

composites hot-pressed at 1800 °C are also plotted for comparison.

This calculation agreed with the experimental results. Therefore, the main cause of the increase in strength in the thin range of the sialon layer is thought to be the compressive residual stress in the sialon layer. However, the strength of the composites hot-pressed at 1900 °C is much higher than that at 1800 °C in the 250–300 μm range of sialon thickness. This unexpected effect is estimated to be attributable to the other reasons, because the elastic constants and the thermal expansion coefficient of 1900 °C sialon are not thought to differ markedly from those of 1800 °C sialon. One of the reasons is thought to be the deep diffusion of yttrium into the sialon layer, because a small amount of Y_2O_3 addition into sialon raises the room-temperature strength [30]. In viewing Fig. 4, the yttrium concentrations in the sialon layer at 250–300 μm from the interface were much higher in the 1900 °C sample than in the 1800 °C sample.

4. Conclusions

1. The fracture strength was almost constant with decreasing thickness from 1300 μm to approximately 500 μm, and then increased as the thickness decreased further. The strength of the samples hot-pressed at 1900 °C reached the same level as Si_3N_4 (inner layer) when the sialon thickness was 250–300 μm.

2. No specific fracture morphologies were recognized around the interface between sialon and Si_3N_4.

3. Aluminium concentration changed sharply around the interface, while the yttrium tended to diffuse deeper than aluminium. This tendency was remarkable in the samples hot-pressed at 1900 °C.

4. The existence of compressive residual stress in the sialon layer was revealed and the compressive residual stress increased as the sialon thickness decreased down to 250–300 μm.

5. The increase in strength with decrease in sialon thickness in the samples hot-pressed at 1800 °C approximately agreed with the prediction based on the mechanical calculations in which the residual stress was considered. However, the strength of the samples hot-pressed at 1900 °C was much higher than the prediction in the 250–300 μm range of the sialon thickness.

Acknowledgements

This work has been entrusted by NEDO as part of the Synergy Ceramics Project under the Industrial Science and Technology Frontier (ISTF) Program promoted by AIST, MITI, Japan. The authors are member of the Joint Research Consortium of Synergy Ceramics.

References

1. G. ZIEGLER, J. HEINRICH and G. WÖTTING, *J. Mater. Sci.* **22** (1987) 3041.
2. J. WEISS, *Ann. Rev. Mater. Sci.* **11** (1981) 381.
3. T. EKSTRÖM and M. NYGREN, *J. Amer. Ceram. Soc.* **75** (1992) 259.
4. K. H. JACK, *J. Mater. Sci.* **11** (1976) 1135.
5. K. H. JACK and W. I. WILSON, *Nature (Lond.) Phys. Sci.* **238** (1977) 28.
6. J. S. MOYA, R. MORENO and J. REQUENA, *J. Eur. Ceram.* **7** (1991) 27.
7. J. REQUENA, R. MORENO and J. S. MOYA, *J. Amer. Ceram. Soc.* **72** (1989) 1511.
8. H. WOHLFROMM, P. PENA, J. S. MOYA and J. REQUENA, *ibid.* **75** (1992) 3474.
9. R. MORENO, A. J. SANCHEZ-HERENCIA and J. S. MOYA, in "Functionally Gradient Materials" (Ceramic Transactions **42**) edited by J. B. Holt, M. Koizumi, T. Hirai and Z. A. Munir (American Ceramic Society, Columbus, OH, 1993) p. 149.
10. J. REQUENA, J. S. MOYA and P. PENA, *ibid.* p. 203.
11. D. B. MARSHALL, *Amer. Ceram. Soc. Bull.* **71** (1992) 969.
12. D. B. MARSHALL, J. J. RATTO and F. F. LANGE, *J. Amer. Ceram. Soc.* **74** (1991) 2979.
13. W. J. CLEGG, K. KENDALL, N. MĆN. ALFORD, T. W. BUTTON and J. D. BIRCHALL, *Nature* **347** (1990) 455.
14. H. KATSUKI, H. ICHINOSE, A. SHIRAISHI, H. TAKAGI and Y. HIRATA, *J. Ceram. Soc. Jpn.* **101** (1993) 1068.
15. R. A. CUTLER, J. D. BRIGHT, A. V. VIRKAR and D. K. SHETTY, *J. Amer. Ceram. Soc.* **70** (1987) 714.
16. A. V. VIRKAR, J. L. HUANG and R. A. CUTLER, *J. Amer. Ceram. Soc.* **70** (1987) 164.
17. A. V. VIRKAR, J. F. JUE, J. J. HANSEN and R. A. CUTLER, *ibid.* **71** (1988) C148.
18. R. SATHYAMOORTHY, A. V. VIRKAR and R. A. CUTLER, *ibid.* **75** (1992) 1136.
19. Y. GOTO, T. YONEZAWA, A. TSUGE and M. KOMATSU, in "Proceedings of the 3rd Fall Symposium of the Ceramic Society of Japan, edited by N. Mizutani (Ceramic Society of Japan, Tokyo, 1990) p. 148.
20. M. ASAYAMA, T. KAMEDA and M. KOMATSU, *ibid.*, p. 92.
21. M. ASAYAMA and T. KAMEDA, *FC Report* **10** (1992) 267.
22. A. TSUGE and K. NISHIDA, *Amer. Ceram. Soc. Bull.* **57** (1978) 424.
23. A. TSUGE, K. NISHIDA and M. KOMATSU, *J. Amer. Ceram. Soc.* **58** (1975) 323.
24. B. D. CULLITY, "Elements of X-Ray Diffraction" (Addison-Wesley, Reading, MA, 1978) p. 447.
25. H. IWASAKI, in "Mechanical Properties of Ceramics", edited by T. Hanazawa (Ceramic Society of Japan, Tokyo, 1979) p. 115.
26. Y. S. TOULOUKIAN, R. K. KIRBY, R.E. TAYLOR and T. Y. LEE, "Thermal Expansion of Nonmetallic Solids" (IFI/Prenum, New York, 1977) p. 19.
27. H. ABE, in "Mechanical Properties of Ceramics", edited by T. Hanazawa (Ceramic Society of Japan, Tokyo, 1979) p. 174.
28. A. ATSUMI, K. SUZUKI and K. MIKATA, "Strength of Materials" (Morikita Shuppan, Tokyo, 1976) p. 61.
29. A. ATSUMI, K. SUZUKI and K. MIKATA, *ibid.*, p. 124.
30. T. EKSTRÖM, P. O. KÄLL, M. NYGREN and P. O. OLSSON, *J. Mater. Sci.* **24** (1989) 1853.

Received 23 July 1996
and accepted 22 August 1997